

Strong unitary and overlap uncertainty relations: theory and experiment

Kok-Wei Bong,¹ Nora Tischler,¹ Raj B. Patel,¹ Sabine Wollmann,^{1,2} Geoff J. Pryde,^{1,*} and Michael J. W. Hall¹

¹*Centre for Quantum Computation and Communication Technology (Australian Research Council),
Centre for Quantum Dynamics, Griffith University, Brisbane, QLD 4111, Australia.*

²*Quantum Engineering Technology Labs, H. H. Wills Physics Laboratory and
Department of Electrical & Electronic Engineering, University of Bristol, BS8 1FD, UK.*

We theoretically and experimentally investigate a strong uncertainty relation valid for any n unitary operators, which implies the standard uncertainty relation as a special case, and which can be written in terms of geometric phases. It is saturated by every pure state of any n -dimensional quantum system, generates a tight overlap uncertainty relation for the transition probabilities of any $n + 1$ pure states, and gives an upper bound for the out-of-time-order correlation function. We test these uncertainty relations experimentally for photonic polarisation qubits, including the minimum uncertainty states of the overlap uncertainty relation, via interferometric measurements of generalised geometric phases.

Introduction.— Uncertainty relations set fundamental limits on what is possible in a quantum world, with implications ranging from bounds in quantum metrology [1, 2] to the security of quantum cryptographic schemes [3, 4]. Preparation uncertainty relations, for example, limit the degree to which properties of a quantum system can be simultaneously specified. We obtain a simple, but powerful, preparation uncertainty relation that places lower bounds on the uncertainties of any given set of n unitary operators, and which unifies, generalises, and significantly strengthens previous results. This unitary uncertainty relation is saturated by all pure states of any d -dimensional Hilbert space with $d \leq n$; is invariant under the rescaling of operators by arbitrary phase factors; generalises a recent uncertainty relation for two unitary operators [5, 6]; and is strictly stronger than the standard Robertson-Schrödinger uncertainty relation [7, 8].

Overlap uncertainty relations reflect the nonclassical property that even pure quantum states typically overlap, important for quantum state discrimination and quantum metrology [1, 2, 9, 10], and in SWAP-tests [11] for quantum communication [12]. For example, the overlap between two phase-shifted optical modes $|\psi\rangle$ and $e^{-iN\chi}|\psi\rangle$ is $|\langle\psi|e^{-iN\chi}|\psi\rangle|^2 = 1 - \chi^2(\Delta N)^2 + O(\chi^4)$, implying that a small overlap, as required to resolve a small phase shift χ , requires a large photon number uncertainty $\Delta N \gtrsim 1/\chi$. Our unitary uncertainty relation connects quantum limits on state preparation and overlap by generating a tight overlap uncertainty relation for the overlaps of any given set of $n + 1$ pure states.

We experimentally investigate these unitary and overlap uncertainty relations, including minimum uncertainty states of the latter, for polarisation qubits. Our experimental method relies on interferometric measurements of generalised geometric phases [13–15]. It is notable in not requiring pure states, nor prior knowledge of the unitary operators, nor state tomography, in contrast to a recent qutrit experiment [16]. We also apply the unitary uncertainty relation to obtain an upper bound on information scrambling via the out-of-time-order correlator [17–19].

Unitary uncertainty relation.— For n unitary operators U_1, U_2, \dots, U_n and quantum state ρ , define $U_0 = I$ and $v^{(j)} = U_j \rho^{1/2}$. Now, for any given set of $n + 1$ vectors $\{v^{(j)}\}$ with inner product (\cdot, \cdot) , the corresponding Gram matrix G , with coefficients $G_{jk} = (v^{(j)}, v^{(k)})$, is positive semidefinite [20]. Hence, choosing the inner product $(A, B) = \text{Tr}[A^\dagger B]$ on the vector space of linear operators, one has the unitary uncertainty relation (UUR)

$$\det G \geq 0, \quad G_{jk} := \text{Tr}[\rho U_j^\dagger U_k] = \langle U_j^\dagger U_k \rangle. \quad (1)$$

We note that a similar method was used by Robertson to obtain an uncertainty relation for n Hermitian operators and a pure state [21]. For $n = 2$ the UUR reduces to

$$\text{Var } U \text{ Var } V \geq |\langle U^\dagger V \rangle - \langle U^\dagger \rangle \langle V \rangle|^2 \quad (2)$$

for two unitary operators U and V , recently obtained elsewhere by less simple means [5, 6], where the variance of unitary operator U is defined by $\text{Var } U := 1 - |\langle U \rangle|^2$ [22]. The $n = 3$ case is discussed in the Supplemental Material [23]. It is also shown there that expanding $U = e^{i\epsilon A}, V = e^{i\epsilon B}$ in ϵ in Eq. (2) yields the well known Robertson-Schrödinger uncertainty relation [7, 8]

$$\text{Var } A \text{ Var } B \geq \frac{1}{4} |\langle [A, B] \rangle|^2 + \text{Cov}(A, B)^2, \quad (3)$$

for two observables represented by Hermitian operators A and B , where the quantum covariance is defined by $\text{Cov}(A, B) := \frac{1}{2} \langle AB + BA \rangle - \langle A \rangle \langle B \rangle$. Hence, the Robertson-Schrödinger relation follows from the UUR.

To determine the minimum uncertainty states of the UUR, note that the determinant of a Gram matrix vanishes if and only if the vectors $v^{(j)}$ are linearly dependent [20]. For a pure state $\rho = |\psi\rangle\langle\psi|$ this is equivalent to linear dependence of $|\psi\rangle, U_1|\psi\rangle, \dots, U_n|\psi\rangle$, which is always satisfied for the case of a Hilbert space with dimension $d \leq n$. Hence, *every* pure state is a minimum uncertainty state for this case, emphasising the strength of the UUR. In particular, Eq. (1), and hence Eqs. (2)

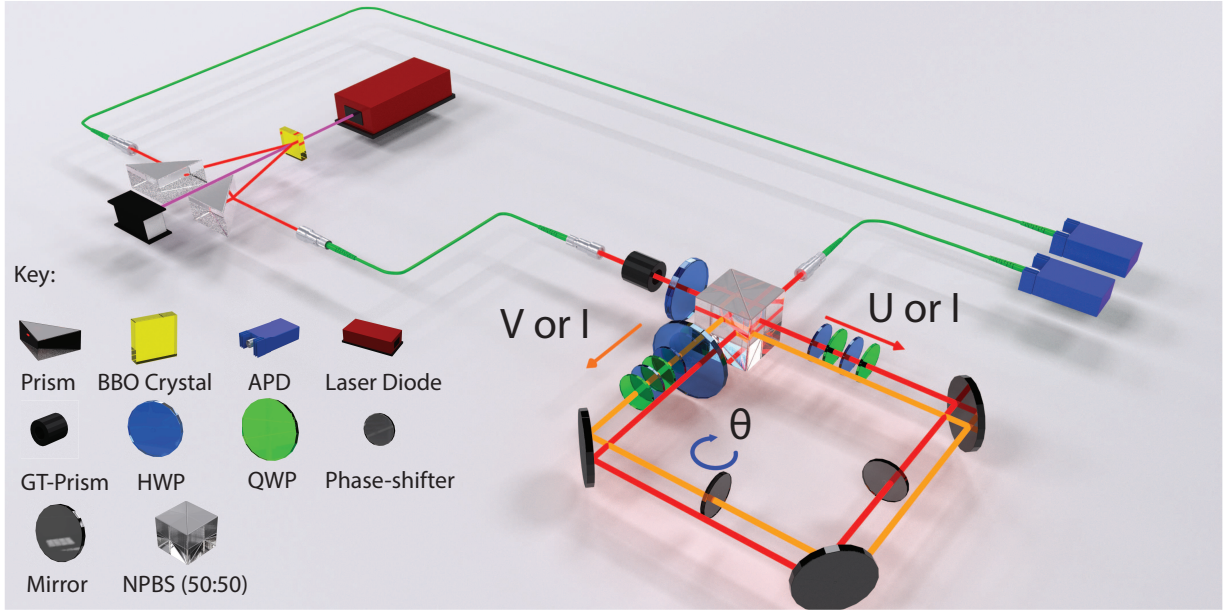


Figure 1. Experimental setup for testing the unitary and overlap uncertainty relations. Pairs of single photons are generated via SPDC using a type-I BBO crystal. The signal photon is prepared in an arbitrary linear polarisation state using a Glan-Taylor (GT) prism followed by a half-waveplate (HWP). After entering a displaced Sagnac interferometer at a 50:50 non-polarising beamsplitter (NPBS), the photon traverses the interferometer in a superposition of the transmitted (red) and reflected (orange) paths. Unitary operators U , V and I are implemented using HWPs and quarter-waveplates (QWP). An additional HWP compensates for the birefringent phase upon reflection at the NPBS. A glass element in one path is tilted to act as a phase-shifter, while a fixed element in the other path keeps the path-length difference to within the coherence length. Two avalanche photodiodes (APDs) detect the signal and idler (heralding) photons.

and (3), are saturated by all qubit pure states. Conversely, a mixed qubit state is a minimum uncertainty state of Eq. (2) if and only if $[U, V] = 0$, i.e., if and only if U and V correspond to rotations about the same axis of the Bloch sphere (see Supplemental Material [23]).

The UUR is invariant under $U_j \rightarrow e^{i\phi_j} U_j$ (even though G_{jk} in Eq. (1) is not), and thus respects the physical equivalence of unitary transformations [23]. Indeed, for a pure state $|\psi\rangle$, Eq. (1) can be explicitly rewritten in terms of the Bargmann projective invariants $B_{j_1 \dots j_r} := \text{Tr} [|\psi_{j_1}\rangle\langle\psi_{j_1}| \dots |\psi_{j_r}\rangle\langle\psi_{j_r}|]$, where $|\psi_{j+1}\rangle := U_j |\psi\rangle$ [14, 23] (these invariants are closely related to geometric phases [15]). For example, Eq. (2) becomes

$$\cos \Phi \geq \frac{T_{12} + T_{13} + T_{23} - 1}{2\sqrt{T_{12}T_{13}T_{23}}}, \quad (4)$$

where $T_{jk} = |\langle\psi_j|\psi_k\rangle|^2 = B_{jk}$ is the transition probability between $|\psi_j\rangle$ and $|\psi_k\rangle$, and Φ is the phase of B_{123} . The saturation of this inequality for all pure qubit states corresponds to an identity in spherical trigonometry [23, 24]. For general mixed states, the UUR can be tested via the measurement of suitably generalised Bargmann invariants, as reported below. In particular, Eq. (2) is equivalent to

$$\cos \Phi \geq \frac{|\langle U \rangle|^2 + |\langle V \rangle|^2 + |\langle U^\dagger V \rangle|^2 - 1}{2|\langle U \rangle \langle U^\dagger V \rangle \langle V^\dagger \rangle|}, \quad (5)$$

generalising Eq.(4), where Φ is the phase of the generalised Bargmann invariant $\langle U \rangle \langle U^\dagger V \rangle \langle V^\dagger \rangle$ [23].

Overlap uncertainty relation.— As previously noted, the generic overlapping of quantum states is important in quantum state discrimination, quantum metrology and quantum communication [1, 2, 9, 10, 12]. A simple example of an overlap uncertainty relation is $\sqrt{1 - T_{12}} \geq \sqrt{1 - T_{13}} + \sqrt{1 - T_{23}}$, for the transition probabilities of any three pure states $|\psi_1\rangle, |\psi_2\rangle, |\psi_3\rangle$, corresponding to the triangle inequality for trace distance [10]. However, noting that $\cos \Phi \leq 1$, Eq. (4) immediately yields the stronger overlap uncertainty relation (OUR),

$$T_{12} + T_{13} + T_{23} - 2\sqrt{T_{12}T_{13}T_{23}} \leq 1. \quad (6)$$

This relation is tight, being saturated if and only if the states lie on a geodesic in Hilbert space, and for qubits corresponds to their Bloch vectors lying on a great circle [23]. For states $|\psi\rangle, U|\psi\rangle, V|\psi\rangle$, with fixed U and V , saturation of the OUR determines the corresponding minimum uncertainty states $\{|\psi\rangle\}$, as investigated experimentally below. More generally, the UUR (1) generates an overlap uncertainty relation for $n + 1$ states, explored further in the Supplemental Material [23].

Experimental setup.— Our experiment uses polarisation states of single photons and a displaced Sagnac interferometer with controllable unitary transformations,

U in the transmitted arm and V in the reflected arm (see Fig. 1). We can determine the value of $\langle U^\dagger V \rangle$ for an input state ρ by first noting that the average output photon number is given by $\langle N \rangle_\chi = \frac{1}{2} [1 + \text{Re} \{ e^{-i\chi} \langle U^\dagger V \rangle \}]$, where χ is the phase difference between the two arms. Hence, we can obtain an interference pattern by varying χ , with associated visibility

$$\mathcal{V}(U, V) := \frac{\langle N \rangle_{\max} - \langle N \rangle_{\min}}{\langle N \rangle_{\max} + \langle N \rangle_{\min}} = |\langle U^\dagger V \rangle|. \quad (7)$$

The values of $|\langle U \rangle|$ and $|\langle V \rangle|$ are similarly determined from the corresponding visibilities $\mathcal{V}(U, I), \mathcal{V}(I, V)$, where I denotes the identity transformation. Further, the phase of $\langle U^\dagger V \rangle$ corresponds to the value of the phase difference χ that gives maximum average output photon number (for a pure input state $|\psi\rangle$ this value is the Pancharatnam phase between $U|\psi\rangle$ and $V|\psi\rangle$ [13, 25]). If $\chi(U, V)$ denotes the location of the interference maximum relative to some fixed phase reference value χ_0 , it follows that the phase of $\langle U^\dagger V \rangle$ is given by

$$\arg \langle U^\dagger V \rangle = \chi(U, V) - \chi(I, I). \quad (8)$$

Thus, our setup allows us to extract $\langle U^\dagger V \rangle$ from the interference pattern via Eqs. (7) and (8). More generally, this setup allows the Gram matrix coefficients G_{jk} in Eq. (1) to be experimentally determined for any set of unitary transformations $U_0 = I, U_1, \dots, U_n$ and polarisation state ρ , and hence the testing of the UUR for any n . We note that, in comparison, a recent qutrit experiment to test the $n = 2$ UUR requires preparation of a strictly pure state $|\psi\rangle$, prior knowledge of the unitary operators (to implement both V and V^\dagger), and tomographic reconstruction of $|\psi\rangle$, $U|\psi\rangle$ and $V|\psi\rangle$ [16].

As shown in Fig. 1, the main component of our setup is the displaced Sagnac interferometer, which is used to measure visibilities and phases as above. For the single-photon source, we use a 410 nm continuous-wave diode laser to pump an optically nonlinear beta Barium Borate (BBO) crystal. The degenerate photon pairs generated by the non-collinear type-I spontaneous parametric down conversion (SPDC) are collected into optical fibres. The idler photon heralds the presence of a signal photon. A half-waveplate (HWP) allows for a range of polarisation qubit states to be encoded on the signal photon, which is then sent into the interferometer. Each unitary operator, U and V , is implemented by a combination of HWPs and quarter-waveplates (QWP), arranged in a group of four: HWP/QWP/HWP/QWP (Fig. 1), with the QWPs set to 45° and the HWPs at variable angles α and β . The condition $\alpha = 90^\circ$ and $\beta = 0^\circ$ corresponds to implementing the identity operation. To realise an adjustable phase shift, a glass element is mounted on a motorised tilt controller and inserted in one arm of the interferometer. A fixed glass element is positioned in the other arm in order to keep the path-length differences to within the coher-

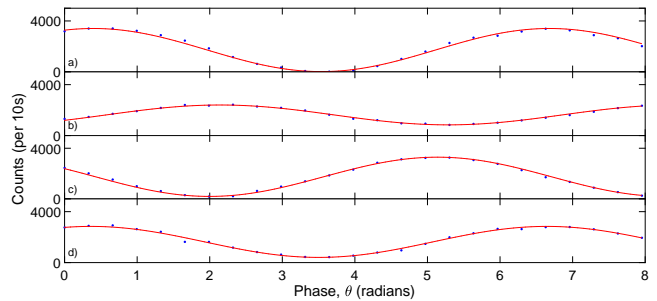


Figure 2. Interferograms as recorded by measuring coincidence counts as a function of the applied phase shift. Unitaries U , V or I are applied to each arm of the Sagnac interferometer as follows a) Transmitted: I , Reflected: I . b) Transmitted: U , Reflected: I . c) Transmitted: I , Reflected: V . d) Transmitted: U , Reflected: V . The $|\langle U^\dagger V \rangle|$ terms or transition probabilities in the uncertainty relations can be calculated from the visibilities of the curves via Eq. (7), and the Bargmann phase via the phase terms in Eq. (9), each of which is determined from the phase of a fringe pattern.

ence length. Finally the photons are detected by silicon avalanche photodiodes.

Results.— The interference fringes in Fig. 2 are obtained by measuring the photon counts at the output of the interferometer. The waveplates in one arm of the interferometer are rotated to produce either the identity operation I or an operation $U(\alpha_U, \beta_U)$ specified by α_U and β_U . Similarly, $V(\alpha_V, \beta_V)$ or I can be implemented in the other arm. The left- and right-hand sides of the UUR in Eq. (5) are calculated by measuring four interference fringes, as shown in Fig. 2. We extract the phase and the visibility of the interference fringes by fitting the data to $A_1 + A_2 \cos^2[\frac{1}{2}(\theta - \theta_0)]$, where $\theta = \chi - \chi_0$ is the controlled phase shift implemented by the tilted glass element. The visibility is then given by $\mathcal{V}(U, V) = A_2/(2A_1 + A_2)$, and $\chi(U, V)$ by θ_0 . The phase Φ of the generalised Bargmann invariant $\langle U \rangle \langle U^\dagger V \rangle \langle V^\dagger \rangle$ follows via Eq. (8) as

$$\Phi = \chi(U, V) - \chi(U, I) - \chi(I, V) + \chi(I, I). \quad (9)$$

Verification of the UUR in Eq. (5) can be seen in Fig. 3. Here, we fix the input state to be horizontally polarised, $|H\rangle$. We vary U and V pairwise in steps such that the full range of $\cos \Phi$ is sampled and, at each setting, the tips of the Bloch vectors for $\{|H\rangle, U|H\rangle, V|H\rangle\}$ form an equilateral spherical triangle. This corresponds to $T_{12} = T_{23} = T_{13}$ in Eq. (4). Saturation of Eq. (4) by pure qubit states corresponds to the area of the triangle being equal to $\Phi/2$ [15, 23, 26, 27]). In practice, there are small experimental imperfections. Although the states have high purity they are not completely mixture free, and so Eq. (5) replaces Eq. (4) as the relevant UUR; also the nominal equilateral configuration is not exact. Nevertheless, since $|\langle U \rangle|^2 \approx |\langle V \rangle|^2 \approx |\langle U^\dagger V \rangle|^2$, we write the average of these quantities as T , which forms the

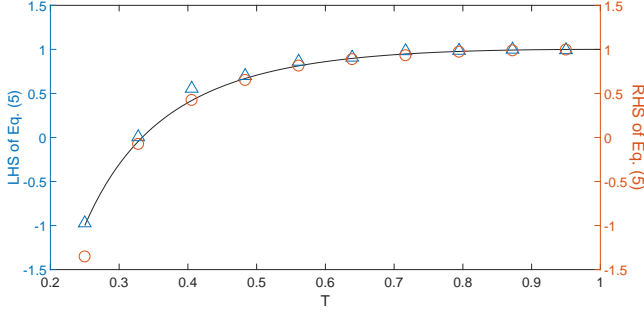


Figure 3. Verification of the UUR in the form of Eq. (5), and its saturation by a pure qubit state. Using a fixed input state, U and V are varied pairwise over a range as described in the text. At each step, parameterised by the mod-squared expectation value T of the operators, the left-hand (blue triangles) and right-hand (red circles) sides of the UUR are determined from experimental measurements. The black line represents the theoretical prediction for saturation of Eq. (5). The errors, calculated from the standard errors of the fit parameters, are smaller than the size of the data points.

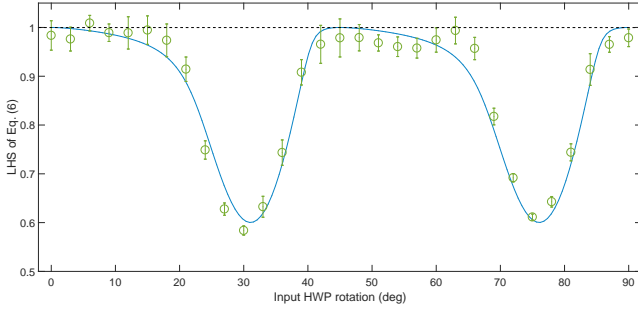


Figure 4. Experimental test of the OUR in Eq. (6). The unitary operators in both arms of the interferometer remain fixed and we input a family of states lying in the linear polarisation plane. The green data points represent the left-hand side of Eq. (6). The blue solid line represents the theoretical curve of the left-hand side of Eq. (6). Minimum uncertainty states correspond to a value of unity, which is marked by the black dashed line. The error bars are calculated from the standard errors of the fit parameters.

x-axis in Fig. 3. In the ideal pure state case for this configuration, $T = T_{ij}$ ($\forall i \neq j$) and $T_{12} = |\langle U \rangle|^2$, etc.

The experimental procedure to test the OUR in Eq. (6) uses a set of linearly polarised input states of high purity, and fixed $U(\alpha_U = 36^\circ, \beta_U = 0^\circ)$ and $V(\alpha_V = 0^\circ, \beta_V = 36^\circ)$. The transition probabilities in Eq. (6) may be determined from the measured visibilities in Eq. (7), via $T_{jk} = |\langle U_j^\dagger U_k \rangle|^2 = \mathcal{V}(U_j, U_k)^2$ for a pure input state. The results are shown in Fig. 4. The minimum uncertainty states correspond to the upper bound of unity in Eq. (6). We note that one of the sources of error in our experiments is the imperfect calibration and retardation of the waveplates, which leads to the implemented unitary operations deviating slightly from the expected settings.

Out-of-time-order correlators.— The UUR may also be used to obtain a bound for the out-of-time-order correlator (OTOC), $F = \langle W_t^\dagger V^\dagger W_t V \rangle$, for a fixed unitary V and time-dependent unitary W_t . The OTOC determines the disturbance caused by V on a later measurement of W , and is of interest in quantum thermalisation, chaos and information scrambling, both in many body and black hole physics [17–19]. It has only very recently been experimentally measured for some systems [28–30].

In particular, the UUR in Eq. (2) implies $(1 - u^2)(1 - v^2) \geq (|\langle U^\dagger V \rangle| - uv)^2$, with $u = |\langle U \rangle|$, $v = |\langle V \rangle|$, yielding

$$|\langle U^\dagger V \rangle| \leq uv + \sqrt{(1 - u^2)(1 - v^2)} = \cos(\theta_U - \theta_V), \quad (10)$$

with $\theta_U := \cos^{-1} |\langle U \rangle|$. Replacing U by $W_t V$ and V by $V W_t$ then gives the upper bound

$$|F| = |\langle W_t^\dagger V^\dagger W_t V \rangle| \leq \cos(\theta_{V W_t} - \theta_{W_t V}) \quad (11)$$

for the modulus of the OTOC, which shows that $|F|$ is a direct signature of the noncommutativity of V and W_t . Indeed, using $\text{Re}\{F\} \leq |F|$ yields the lower bound

$$\langle [V, W_t]^2 \rangle = 2(1 - \text{Re}\{F\}) \geq 4 \sin^2 \left(\frac{\theta_{V W_t} - \theta_{W_t V}}{2} \right). \quad (12)$$

For polarisation qubits we note that the values of $\theta_{V W_t}$ and $\theta_{W_t V}$ could be obtained from interferometer visibilities corresponding to $|\langle V W_t \rangle|$ and $|\langle W_t V \rangle|$, via Eq. (7), with a time-dependent unitary in one arm.

Conclusion.— We have presented a strong and very general unitary uncertainty relation (UUR), which implies the Robertson-Schrödinger relation and generates a tight state overlap uncertainty relation. We tested these experimentally using polarisation qubit states in an interferometric configuration. This allowed for measurements that led directly to the quantities in the relation, and directly revealed the role of geometric phase in the UUR. We note that the UUR does not assume or require pure states, making it a general and powerful tool for real-world quantum systems.

We expect that the strength of the general UUR in Eq. (1) will lead to further results that enhance and unify quantum uncertainty relations. For example, noting that spin-1/2 observables are both Hermitian and unitary, the UUR in Eq. (2) leads directly to, and hence encompasses, a tight state-independent qubit uncertainty relation obtained recently in Refs. [31, 32] (see Supplemental Material [23]). It would also be of interest in future work to investigate possible connections of the UUR with measurement-disturbance and joint-measurement uncertainty relations; to test the UUR and OUR for higher values of n ; and to implement similar tests of the OTOC bounds in Eqs. (11) and (12) above.

This work was supported by the ARC Centre of Excellence CE110001027. S. W. acknowledges financial support through an Australian Government Research Training Program Scholarship.

* g.pryde@griffith.edu.au

- [1] S. L. Braunstein and C. M. Caves, Phys. Rev. Lett. **72**, 3439 (1994)
- [2] S. L. Braunstein, C. M. Caves, and G. J. Milburn, Ann. Phys. **247**, 135 (1996)
- [3] M. Berta, M. Christandl, R. Colbeck, J. M. Renes, R. Renner, Nature Phys. **6**, 659 (2010)
- [4] M. Tomamichel and R. Renner, Phys. Rev. Lett. **106**, 110506 (2011)
- [5] M. J. W. Hall, A. K. Pati and J. Wu, Phys. Rev. A **93**, 052118 (2016)
- [6] S. Bagchi and A. K. Pati, Phys. Rev. A **94**, 042104 (2016)
- [7] H. P. Robertson, Phys. Rev. **35**, 667A (1930)
- [8] E. Schrödinger, Ber. Kgl. Akad. Wiss. Berlin **24** 296 (1930)
- [9] S. M. Barnett and S. Croke, Adv. Opt. Photonics **1**, 238 (2009)
- [10] M. M. Wilde, *Quantum Information Theory*, 2nd edn (Cambridge University Press, UK, 2017), chap. 9
- [11] R. B. Patel, J. Ho, F. Ferreyrol, T. C. Ralph, G. J. Pryde, Sci. Adv. **2**, e1501531 (2016)
- [12] H. Buhrman, R. Cleve, J. Watrous, and R. de Wolf, Phys. Rev. Lett. **87**, 167902 (2001)
- [13] S. Pancharatnam, Proc. Ind. Acad. Sci. A **54** 247 (1956)
- [14] V. Bargmann, J. Math. Phys. **5**, 862 (1964)
- [15] N. Mukunda and R. Simon, Ann. Phys. **228**, 205 (1993)
- [16] L. Xiao, K. Wang, X. Zhan, Z. Bian, J. Li, Y. Zhang, P. Xue, and A. K. Pati, Optics Express **25**, 17904 (2017)
- [17] P. Hosur, X.-L. Qi, D. A. Roberts, and B. Yoshida, J. High Energy Phys. **2016**, 4 (2016)
- [18] J. Maldacena, S. H. Shenker, and D. Stanford, J. High Energy Phys. **2016**, 106 (2016)
- [19] B. Swingle, G. Bentsen, M. Schleier-Smith, and P. Hayden, Phys. Rev. A **94**, 040302 (2016)
- [20] P. D. Lax, *Linear Algebra and its Applications*, 2nd edn (Wiley, New Jersey, 2007), chap. 10
- [21] H. P. Robertson, Phys. Rev. **46**, 794 (1934)
- [22] J.-M. Levy-Leblond, Ann. Phys. **101**, 319 (1976)
- [23] See Supplemental Material for detailed properties of the unitary and overlap uncertainty relations
- [24] I. Todhunter, *Spherical Trigonometry*, 5th edn (Macmillan, London, 1886), Section 103; also available online from Project Gutenberg
- [25] J. C. Laredo, O. Ortíz, R. Weingärtner, and F. De Zela, Phys. Rev. A **80** 012113 (2009)
- [26] M. V. Berry, Proc. R. Soc. Lond. A **392**, 45 (1984)
- [27] Y. Aharonov and J. Anandan, Phys. Rev. Lett. **58**, 1593 (1987)
- [28] J. Li, R. Fan, H. Wang, B. Ye, B. Zeng, H. Zhai, X. Peng, and J. Du, Phys. Rev. X **7**, 031011 (2017)
- [29] M. Gärttner, J. G. Bohnet, A. Safavi-Naini, M. L. Wall, J. J. Bollinger, and A. M. Rey, Nat. Phys. **13**, 781 (2017)
- [30] E. J. Meier, J. Ang'ong'a, F. A. An, and B. Gadway, Eprint arXiv:1705.06714 [cond-mat.quant-gas] (2017)
- [31] J.-L. Li and C.-F. Qiao, Sci. Rep. **5**, 12708 (2015)
- [32] A. A. Abbott, P.-L. Alzieu, M. J. W. Hall and C. Branciari, Mathematics **4**, 8 (2016)

SUPPLEMENTAL MATERIAL

I. PROPERTIES OF THE UNITARY UNCERTAINTY RELATION

A. An alternate proof

We start by giving an alternate proof of the UUR in Eq. (1) of the main text, using a matrix of operators. First, for a pure state $|\psi\rangle\langle\psi|$ and unitaries $U_0 = I, U_1, U_2, \dots, U_n$, define the kets $|\psi_j\rangle := U_j|\psi\rangle$. Defining the Gram matrix $G(\psi)$ via the coefficients $G_{jk}(\psi) := \langle\psi_j|\psi_k\rangle$, it immediately follows that

$$G(\psi) \geq 0. \quad (\text{S.1})$$

This already implies the UUR for the case of pure states. Note that it can also be written in matrix operator form as

$$\hat{G} \geq 0, \quad \hat{G}_{jk} := U_j^\dagger U_k. \quad (\text{S.2})$$

It follows from either of the above two equations that

$$G(\rho) \geq 0, \quad G(\rho) := \sum_k p_k G(\psi_k) = \text{Tr} [\rho \hat{G}], \quad (\text{S.3})$$

for any density operator $\rho = \sum_k p_k |\psi_k\rangle\langle\psi_k|$, yielding the general UUR

$$\det G(\rho) \geq 0 \quad (\text{S.4})$$

as desired.

Note that it is straightforward to formally generalise the UUR to arbitrary (not necessarily Hermitian) operators A_1, A_2, \dots, A_n , with $v^{(j)}$ of the main text and $|\psi_j\rangle$ above replaced by $A_j \rho^{1/2}$ and $A_j |\psi\rangle$, respectively.

B. Deriving the Robertson-Schrödinger relation

For $n = 2$, writing $U_1 = U$ and $U_2 = V$, (S.4) reduces to

$$\begin{vmatrix} 1 & \langle U \rangle & \langle V \rangle \\ \langle U^\dagger \rangle & 1 & \langle U^\dagger V \rangle \\ \langle V^\dagger \rangle & \langle V^\dagger U \rangle & 1 \end{vmatrix} \geq 0, \quad (\text{S.5})$$

which simplifies to

$$\text{Var } U \text{Var } V \geq |\langle U^\dagger V \rangle - \langle U^\dagger \rangle \langle V \rangle|^2 \quad (\text{S.6})$$

as per Eq. (2) of the main text. Choosing $U = e^{i\epsilon A}$ and $V = e^{i\epsilon B}$ for any two Hermitian operators A and B , one has the Taylor expansions

$$U = I + i\epsilon A - \frac{1}{2}\epsilon^2 A^2 + O(\epsilon^3), \quad V = I + i\epsilon B - \frac{1}{2}\epsilon^2 B^2 + O(\epsilon^3),$$

from which it follows that

$$\text{Var } U := 1 - |\langle U \rangle|^2 = \epsilon^2 \text{Var } A + O(\epsilon^3), \quad (\text{S.7})$$

$$\text{Var } V := 1 - |\langle V \rangle|^2 = \epsilon^2 \text{Var } B + O(\epsilon^3), \quad (\text{S.8})$$

and

$$\begin{aligned} |\langle U^\dagger V \rangle - \langle U^\dagger \rangle \langle V \rangle|^2 &= \epsilon^4 |\langle AB \rangle - \langle A \rangle \langle B \rangle|^2 + O(\epsilon^5) \\ &= \epsilon^4 |\text{Re}\{\langle AB \rangle\} - \langle A \rangle \langle B \rangle \\ &\quad + i \text{Im}\{\langle AB \rangle\}|^2 + O(\epsilon^5) \\ &= \epsilon^4 \left(\text{Cov}(A, B)^2 + \frac{1}{4} |\langle [A, B] \rangle|^2 \right) \\ &\quad + O(\epsilon^5). \end{aligned} \quad (\text{S.9})$$

Substituting these results into Eq. (S.6), dividing by ϵ^4 , and taking the limit $\epsilon \rightarrow 0$, then yields the Robertson-Schrödinger uncertainty relation

$$\text{Var } A \text{Var } B \geq \frac{1}{4} |\langle [A, B] \rangle|^2 + \text{Cov}(A, B)^2, \quad (\text{S.10})$$

as per Eq. (3) of the main text. Note that one cannot proceed in the reverse direction, i.e., the UUR is strictly stronger than the Robertson-Schrödinger uncertainty relation. As shown further below, the UUR may also be used to derive a tight state-independent qubit uncertainty relation [31, 32].

C. Minimum uncertainty qubit states

It was shown in the main text that the UUR is saturated by all pure states of any d -dimensional Hilbert space with $d \leq n$. In particular, all qubit pure states are minimum uncertainty states for $n \geq 2$.

More generally, as noted in the main text, the UUR in Eq. (1) of the main text (repeated in Eq. (S.4) above) is saturated if and only if the $n+1$ operators $v^{(j)} = U_j \rho^{1/2}$ are linearly independent. Since there are at most d^2 linearly independent operators in a d -dimensional Hilbert space, this implies in particular that the UUR is saturated by all density operators when $d^2 \leq n$. For qubits, i.e., $d = 2$, this raises the interesting question of whether there are any density operators, apart from pure states, that saturate the UUR for $n = 2$ or $n = 3$.

It turns out that this question has a simple answer when $n = 2$: a non-pure qubit density operator ρ saturates the UUR in Eq. (S.6) if and only if $[U, V] = 0$, i.e., if and only if U and V correspond to rotations about the same axis of the Bloch sphere. Hence, *all* qubit states are minimum uncertainty states of Eq. (S.6) if U and V commute, while only all *pure* qubit states are minimum uncertainty states if they do not.

To prove this result, first note that if ρ is a non-pure qubit state then it is invertible, so that $v^{(j)}$ may be multiplied on the right by $\rho^{-1/2}$. Hence, saturation of Eq. (S.6)

is equivalent to linear independence of the unitary operators I, U, V , i.e., to

$$\alpha I + \beta U + \gamma V = 0 \quad (\text{S.11})$$

for some constants $(\alpha, \beta, \gamma) \neq (0, 0, 0)$. Taking the commutator with U or V leads to $\beta[U, V] = 0 = \gamma[U, V]$. But if β and γ both vanish then the above equation yields $\alpha = 0$. Hence linear independence implies $[U, V] = 0$. Conversely, if U and V commute we have

$$U = e^{i\chi_0}|0\rangle\langle 0| + e^{i\chi_1}|1\rangle\langle 1|, \quad V = e^{i\kappa_0}|0\rangle\langle 0| + e^{i\kappa_1}|1\rangle\langle 1| \quad (\text{S.12})$$

for some qubit basis $\{|0\rangle, |1\rangle\}$ and phases $\chi_0, \chi_1, \kappa_0, \kappa_1$. Substituting into Eq. (S.11) then gives

$$\begin{pmatrix} e^{i\chi_0} & e^{i\kappa_0} \\ e^{i\chi_1} & e^{i\kappa_1} \end{pmatrix} \begin{pmatrix} \beta \\ \gamma \end{pmatrix} = - \begin{pmatrix} \alpha \\ \alpha \end{pmatrix}. \quad (\text{S.13})$$

This clearly has nontrivial solutions $(\alpha, \beta, \gamma) \neq (0, 0, 0)$, corresponding to linear dependence, when the determinant of the matrix on the left-hand side does not vanish, i.e., if $e^{i(\chi_1 - \chi_0)} \neq e^{i(\kappa_1 - \kappa_0)}$. Finally, if the determinant does vanish, then one still has linear dependence since $U = e^{i\phi}V$ in this case (with $\phi = \chi_0 - \kappa_0$).

D. Tight state-independent qubit uncertainty relation

Qubit observables may be represented, up to translation and rescaling, by Hermitian operators of the form $A = \mathbf{a} \cdot \sigma$, where \mathbf{a} is a unit 3-vector and $\sigma \equiv (\sigma_1, \sigma_2, \sigma_3)$ denotes the vector of Pauli operators. It follows that $A^\dagger A = A^2 = I$, i.e., these operators are unitary. Hence the UUR may be directly applied to such observables. Further, noting the above section, the corresponding uncertainty relations are saturated for all pure qubit states.

For example, for $n = 2$ consider the UUR in Eq. (2) of the main text, i.e., as per Eqs. (S.5) and (S.6), for the case of a qubit state $\rho = \frac{1}{2}(I + \mathbf{r} \cdot \sigma)$. Replacing U and V by $A = \mathbf{a} \cdot \sigma$ and $B = \mathbf{b} \cdot \sigma$, respectively, for arbitrary unit directions \mathbf{a}, \mathbf{b} , and using

$$\langle U^\dagger V \rangle = \langle AB \rangle = \mathbf{a} \cdot \mathbf{b} + i(\mathbf{a} \times \mathbf{b}) \cdot \mathbf{r},$$

leads via Eq. (S.5) to

$$\langle A \rangle^2 + \langle B \rangle^2 - 2(\mathbf{a} \cdot \mathbf{b})\langle A \rangle\langle B \rangle \leq 1 - (\mathbf{a} \cdot \mathbf{b})^2 - [(\mathbf{a} \times \mathbf{b}) \cdot \mathbf{r}]^2, \quad (\text{S.14})$$

with equality for pure states, i.e., when $|\mathbf{r}| = 1$. It follows that one has the tight state-independent uncertainty relation

$$\begin{aligned} & (\Delta A)^2 + (\Delta B)^2 + 2|\mathbf{a} \cdot \mathbf{b}|\sqrt{1 - (\Delta A)^2}\sqrt{1 - (\Delta B)^2} \\ & \geq 2 - [\langle A \rangle^2 + \langle B \rangle^2 - 2(\mathbf{a} \cdot \mathbf{b})\langle A \rangle\langle B \rangle] \\ & \geq 1 + (\mathbf{a} \cdot \mathbf{b})^2 + [(\mathbf{a} \times \mathbf{b}) \cdot \mathbf{r}]^2 \\ & \geq 1 + (\mathbf{a} \cdot \mathbf{b})^2, \end{aligned} \quad (\text{S.15})$$

given for particular cases in [31] and more generally in [32].

E. Physical invariance and Bargmann invariants

A unitary transformation U takes any given state ρ to the state $U\rho U^\dagger$. Hence, U and $e^{i\phi}U$ are physically equivalent transformations for any phase ϕ . As remarked in the main text, the general UUR in Eq. (S.4) respects this physical equivalence. In particular, under $U_j \rightarrow e^{i\phi_j}U_j$, it follows from Eqs. (S.2) and (S.3) that

$$G(\rho) \rightarrow KG(\rho)K^\dagger \quad (\text{S.16})$$

where K is the unitary diagonal matrix

$$K := \begin{pmatrix} e^{-i\phi_0} & 0 & \dots & 0 \\ 0 & e^{-i\phi_1} & \dots & 0 \\ \vdots & \vdots & \ddots & \vdots \\ 0 & 0 & \dots & e^{-i\phi_n} \end{pmatrix}. \quad (\text{S.17})$$

Hence the positivity of $G(\rho)$ is preserved (as are its eigenvalues), implying that the UUR respects physical invariance as claimed in the main text.

In fact, the UUR satisfies a stronger form of physical invariance. In particular, expanding the determinant in Eq. (S.4) in the usual way, the UUR can be rewritten as a sum of products,

$$\sum_P (-1)^P \langle U_0 U_{P(0)}^\dagger \rangle \dots \langle U_n U_{P(n)}^\dagger \rangle \geq 0, \quad (\text{S.18})$$

where the sum is over permutations of $\{0, 1, \dots, n\}$ and $(-1)^P$ denotes the sign of permutation P . In each summand, note that U_j and U_j^\dagger will appear exactly once, for each value of j . Hence, each product is invariant under $U_j \rightarrow e^{i\phi_j}U_j$, i.e., each individual term in the above sum respects physical invariance.

This stronger property is closely related to Bargmann invariants [14]. The Bargmann invariant associated with a given set of m pure states $|\psi_1\rangle, \dots, |\psi_m\rangle$ is defined by the cyclic product $B_{12\dots m} := \langle \psi_1 | \psi_2 \rangle \langle \psi_2 | \psi_3 \rangle \dots \langle \psi_m | \psi_1 \rangle$, which is clearly invariant under rephasings $|\psi_j\rangle \rightarrow e^{i\phi_j}|\psi_j\rangle$. Thus it is a projective invariant, as may also be seen by writing it as a trace of a product of projection operators, $B_{1\dots m} = \text{Tr} [|\psi_1\rangle\langle\psi_1| |\psi_2\rangle\langle\psi_2| \dots |\psi_m\rangle\langle\psi_m|]$. Choosing $|\psi_{j+1}\rangle := U_j|\psi_j\rangle$, it follows immediately that the UUR (S.18) can be rewritten as an uncertainty relation for the associated Bargmann invariants.

For example, for $n = 2$ and pure state $\rho = |\psi\rangle\langle\psi|$ the UUR in Eq. (S.5) simplifies to

$$1 - B_{23} - B_{12} - B_{13} + B_{123} + B_{321} \geq 0, \quad (\text{S.19})$$

which is equivalent to Eq. (4) of the main text. Similarly, for $n = 3$ one finds via Eq. (S.18) that the Bargmann invariants associated with any 4 pure states satisfy the

uncertainty relation

$$\begin{aligned}
2 \leq & (1 - B_{12})(1 - B_{34}) + (1 - B_{13})(1 - B_{24}) \\
& + (1 - B_{14})(1 - B_{23}) \\
& + 2 \operatorname{Re} \{B_{123} + B_{124} + B_{134} + B_{234}\} \\
& - 2 \operatorname{Re} \{B_{1234} + B_{1243} + B_{1324}\}. \quad (\text{S.20})
\end{aligned}$$

This relation may equivalently be written as

$$\begin{aligned}
\operatorname{Var} U \operatorname{Var}(V^\dagger W) + \operatorname{Var} V \operatorname{Var}(U^\dagger W) + \operatorname{Var} W \operatorname{Var}(U^\dagger V) \\
\geq 2 - 2 \operatorname{Re} \{B_{123} + B_{124} + B_{134} + B_{234}\} \\
+ 2 \operatorname{Re} \{B_{1234} + B_{1243} + B_{1324}\}, \quad (\text{S.21})
\end{aligned}$$

in terms of the variances of U , V and W , with equality holding for all qubit pure states as per the main text.

More generally, for mixed states the UURs for $n = 2$ and $n = 3$ take exactly the same form as Eqs. (S.19)-(S.21), providing one defines the *generalised* Bargmann invariant by the cyclic product

$$B_{12\dots m} := \langle U_1 U_2^\dagger \rangle \langle U_2 U_3^\dagger \rangle \dots \langle U_m U_1^\dagger \rangle \quad (\text{S.22})$$

for any given set of unitary operators U_1, U_2, \dots, U_m and state ρ . Note that $B_{12\dots m}$ may be measured for polarisation qubits via the interferometric method of the main text. It would be of interest, in the qubit case, to relate Eq. (S.21) to the corresponding state-independent qubit uncertainty relation in Ref. [32] for any three qubit observables.

F. Spherical trigonometry and the geometric phase

The saturation of the UUR in Eq. (4) of the main text by all pure qubit states corresponds to the statement that

$$\cos \Phi = \frac{T_{12} + T_{13} + T_{23} - 1}{2\sqrt{T_{12}T_{13}T_{23}}} \quad (\text{S.23})$$

for the transition probabilities $T_{jk} = |\langle \psi_j | \psi_k \rangle|^2$ of any three qubit states $|\psi_1\rangle, |\psi_2\rangle, |\psi_3\rangle$, where Φ is the phase of the Bargmann invariant $B_{123} = \langle \psi_1 | \psi_2 \rangle \langle \psi_2 | \psi_3 \rangle \langle \psi_3 | \psi_1 \rangle$.

Denoting the angles between the corresponding pairs of Bloch vectors by γ_{jk} then $T_{jk} = \cos^2 \frac{1}{2} \gamma_{jk}$, and the above equality can be rewritten as

$$\cos \Phi = \frac{\cos^2 \frac{1}{2} \gamma_{12} + \cos^2 \frac{1}{2} \gamma_{13} + \cos^2 \frac{1}{2} \gamma_{23} - 1}{2 \cos \frac{1}{2} \gamma_{12} \cos \frac{1}{2} \gamma_{13} \cos \frac{1}{2} \gamma_{23}} = \cos \frac{1}{2} A, \quad (\text{S.24})$$

where A is the area of the spherical triangle formed by the Bloch vectors, and the second equality is an old but little known identity from spherical trigonometry (see Eq. (3) of section 103 of [24]). Thus, saturation of the UUR by qubit states corresponds to the known relation [15]

$$A = 2|\Phi|, \quad (\text{S.25})$$

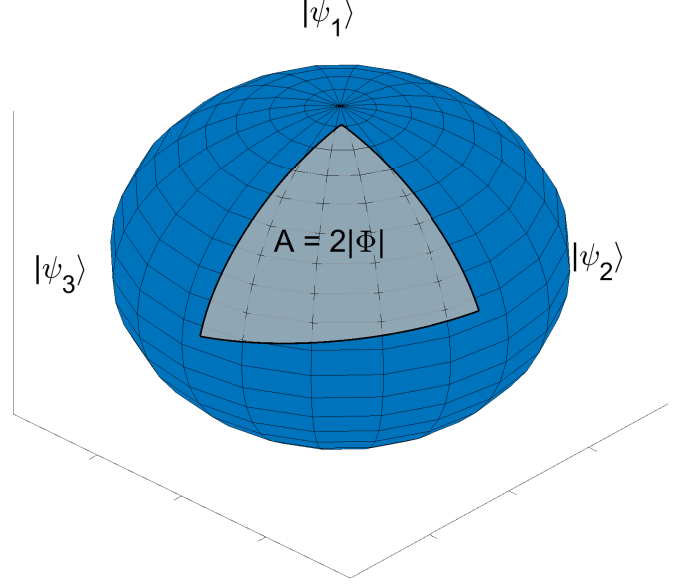


Figure S1. Equality in Eq.(S.23, for any pure qubit states $|\psi_1\rangle, |\psi_2\rangle, |\psi_3\rangle$, corresponds to a simple geometric relation connecting the Bargmann phase Φ of the states to the area A of the corresponding triangle on the Bloch sphere, as per Eq. (S.25).

between Bargmann phase and the area of a spherical triangle, depicted in Fig. S1. This relation is an example of the more general connection between area and geometric phase [15], where evolution of a qubit about a circuit on the Bloch sphere generates a geometric phase equal to half the area enclosed by the circuit [26, 27].

II. PROPERTIES OF THE OVERLAP UNCERTAINTY RELATION

A. Saturation

The overlap uncertainty relation in Eq. (6) of the main text,

$$T_{12} + T_{13} + T_{23} - 2\sqrt{T_{12}T_{13}T_{23}} \leq 1, \quad (\text{S.26})$$

for the transition probabilities of any three pure states $|\psi_1\rangle, |\psi_2\rangle, |\psi_3\rangle$, may be rewritten as

$$\begin{aligned}
1 \geq & \cos^2 \theta_{12} + \cos^2 \theta_{13} + \cos^2 \theta_{23} \\
& - 2 \cos \theta_{12} \cos \theta_{13} \cos \theta_{23}, \quad (\text{S.27})
\end{aligned}$$

where $\theta_{jk} = \cos^{-1} |\langle \psi_j | \psi_k \rangle| \in [0, \pi/2]$ is the angle between states $|\psi_j\rangle$ and $|\psi_k\rangle$. Saturation of this relation corresponds to a quadratic equation for $\cos \theta_{23}$, which is easily solved to give

$$\cos \theta_{23} = \cos(\theta_{12} \pm \theta_{13}). \quad (\text{S.28})$$

It follows, recalling $\theta_{jk} \in [0, \pi/2]$, that

$$\theta_{23} = |\theta_{12} \pm \theta_{13}|, \quad (\text{S.29})$$

i.e., one of $\theta_{23} = \theta_{12} + \theta_{13}$, $\theta_{12} = \theta_{13} + \theta_{23}$, $\theta_{13} = \theta_{12} + \theta_{23}$ must hold. Since the angle between two pure states is a metric (the well-known Fubini-Study metric), it follows from the triangle inequality that saturation corresponds to the states lying on a common geodesic with respect to this metric, as claimed in the main text.

For the case of qubit states, one has the simple relation $\theta_{jk} = \frac{1}{2}\gamma_{jk}$, where $\gamma_{jk} \in [0, \pi]$ is the angle between the corresponding Bloch vectors. Hence, in this case, Eq. (S.29) immediately implies that saturation is equivalent to the Bloch vectors lying on a great semicircle of the Bloch sphere (corresponding to a spherical triangle of area $A = 0$).

B. Minimum uncertainty states for fixed U and V

For pure states $|\psi_1\rangle = |\psi\rangle$, $|\psi_2\rangle = U|\psi\rangle$, $|\psi_3\rangle = V|\psi\rangle$, the overlap uncertainty relation can be rewritten as the uncertainty relation

$$\text{Var } U \text{Var } V \geq (|\langle U^\dagger V \rangle| - |\langle U \rangle| |\langle V \rangle|)^2 \quad (\text{S.30})$$

for the unitary operators U and V . The minimum uncertainty states corresponding to the saturation of this relation are, therefore, those states $|\psi\rangle$ for which $|\psi\rangle, U|\psi\rangle, V|\psi\rangle$ lie on a common geodesic in Hilbert space (see Sec. II A above).

From Eq. (S.29), these states are given by the solutions of

$$\cos^{-1} |\langle \psi | U^\dagger V | \psi \rangle| = |\cos^{-1} |\langle \psi | U | \psi \rangle| \pm \cos^{-1} |\langle \psi | V | \psi \rangle|. \quad (\text{S.31})$$

For qubit minimum uncertainty states, the Bloch vectors of $|\psi\rangle, U|\psi\rangle, V|\psi\rangle$ lie on a great semicircle of the Bloch sphere (see above). Further, note that the angle γ between two unit Bloch vectors \mathbf{a} and \mathbf{b} satisfies $\cos \gamma = \mathbf{a} \cdot \mathbf{b}$. Hence, denoting the Bloch vector of $|\psi\rangle$ by \mathbf{a} and U and V by suitable rotation matrices R_U and R_V , Eq. (S.31) reduces to (recalling $\theta_{jk} = \frac{1}{2}\gamma_{jk}$):

$$\cos^{-1} \frac{\mathbf{a}^\top R_U^\top R_V \mathbf{a}}{2} = \left| \cos^{-1} \frac{\mathbf{a}^\top R_U \mathbf{a}}{2} \pm \cos^{-1} \frac{\mathbf{a}^\top R_V \mathbf{a}}{2} \right|. \quad (\text{S.32})$$

Note that if R_U and R_V correspond to rotations about the unit vectors \mathbf{m} and \mathbf{n} , then $\mathbf{a} = \pm \mathbf{m}$ and $\mathbf{a} = \pm \mathbf{n}$ are solutions of these equations. More generally, since \mathbf{a} has two continuous degrees of freedom, it follows that there will be in general two 1-parameter families of minimum uncertainty states, corresponding to the $+$ and $-$ signs respectively (although more solutions are possible in degenerate cases). A generic example is shown in Fig. S2.

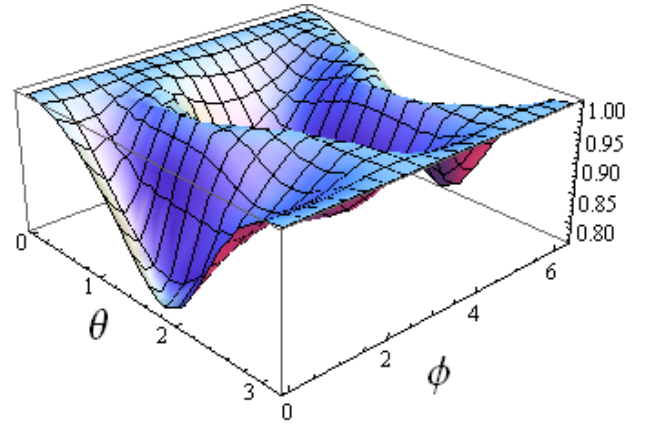


Figure S2. The OUR in Eq. (S.26) for fixed U and V . The Bloch vector of state $|\psi\rangle$ is parameterised by spherical coordinates (θ, ϕ) , and the right-hand side of Eq. (S.26) is shown on the vertical axis. Saturation occurs for minimum uncertainty states, and it is seen from the figure that there are two families of such states, where these correspond to the cases that $|\psi\rangle, U|\psi\rangle$ and $V|\psi\rangle$ lie on a common great semicircle of the Bloch sphere. The choices for U and V in the figure are given by $U = e^{i\pi\sigma_y/8}$ and $V = e^{i\pi\sigma_z/8}$, corresponding to Bloch sphere rotations of $\pi/4$ about the y -axis and z -axis respectively. The minimum uncertainty states correspond to a maximum value of unity. Note that Fig. 4 of the main text corresponds to a vertical cross section of a similar surface.

C. Higher-order OURs

The OUR in Eq. (6) of the main text (see also Eq. (S.27) above) follows from the UUR with $n = 2$. One can similarly obtain OURs corresponding to larger values of n . For example, for $n = 3$, recalling the definition of the Bargmann invariants in Eq. (S.22), and using $\text{Re}\{x + y\} \leq |x| + |y|$, the UUR in Eq. (S.20) immediately yields the OUR

$$\begin{aligned} 1 \leq & \frac{1}{2}(1 - T_{12})(1 - T_{34}) + \frac{1}{2}(1 - T_{13})(1 - T_{24}) \\ & + \frac{1}{2}(1 - T_{14})(1 - T_{23}) \\ & + \sqrt{T_{12}T_{23}T_{13}} + \sqrt{T_{12}T_{24}T_{14}} + \sqrt{T_{13}T_{34}T_{14}} \\ & + \sqrt{T_{23}T_{34}T_{24}} + \sqrt{T_{12}T_{23}T_{34}T_{14}} \\ & + \sqrt{T_{12}T_{13}T_{24}T_{34}} + \sqrt{T_{13}T_{14}T_{23}T_{24}} \end{aligned} \quad (\text{S.33})$$

for the transition probabilities of any 4 pure states.

Note that if $|\psi_4\rangle$ is orthogonal to the first three states, i.e., $T_{j4} = 0$ for $j = 1, 2, 3$, then Eq. (S.33) reduces to the OUR in Eq. (6) of the main text for any 3 pure states. Since the latter can be saturated by suitable qubit states, it follows that the above OUR can be saturated by suitable qutrit states.